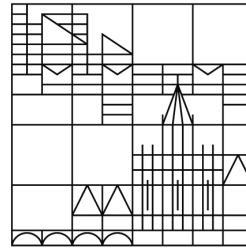


Universität
Konstanz

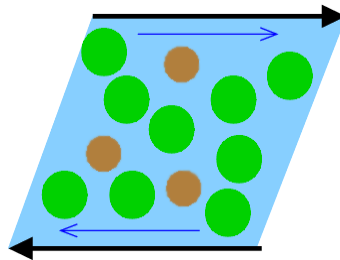


– Bachelorarbeit –

Shear moduli of two dimensional colloidal mixtures

Rabea Seyboldt

August 4, 2011



1. Gutachter: Prof. Dr. Matthias Fuchs

2. Gutachter: Dr. Peter Keim

Betreuer: Fabian Weyßer

Zusammenfassung

In dieser Arbeit wird mit Hilfe der Modenkopplungstheorie (MCT) eine Formel für das Schermodul $G(t)$ für binäre kolloidale Mischungen in zwei Dimensionen aus einer MCT-Formel für drei Dimensionen abgeleitet.

Damit wird das Plateau-Schermodul G_∞ von binären Mischungen harter Kugeln und dipolaren Punktteilchen für verschiedene Zusammensetzungen jeweils am Glasübergang berechnet.

Die Ergebnisse werden einem dreidimensionalen System harter Kugeln gegenübergestellt, dafür werden Werte von Götze und Voigtmann herangezogen. Die Schermoduln $\frac{G_\infty}{nk_B T}$ der drei Systeme haben etwa den selben Wert 20 mit Abweichungen von etwa ± 10 . Dabei ist n die totale Anzahldichte.

Ein Vergleich von zwei- und dreidimensionalem Hartkugel- und zweidimensionalem dipolarem System zeigt, dass alle drei Systeme ihr Maximum des kritischen Parameters und des Plateau-Schermoduls (abhängig vom Größenverhältnis δ und dem Anzahlverhältnis x_s der kleinen Teilchen relativ zu den großen) im Mischungsbereich vieler sehr kleiner Kugeln haben. Eine Analyse der Partikel-Koordinaten ergibt, dass dies zumindest für dipolare Teilchen nicht durch eine Verarmungsattraktion zwischen den großen Kugeln entsteht. Allerdings scheint der Effekt durch ein Störungsfeld der kleinen Partikel auf die großen zustande zu kommen.

Mit Ausnahme dieser Maxima zeigen alle drei Systeme eine Verminderung des Plateau-Schermoduls durch Mischen. Dies kann mit der Plastifizierung von Polymeren verglichen werden.

Die Glasübergangsfläche des kritischen Parameters Γ_c bzw. ϕ_c ergibt, dass in allen drei Systemen der kritische Parameter durch Mischen erhöht, also die Flüssigkeit stabilisiert wird. Für die Hartkugel-Systeme existiert ein Grenzwert für δ über dem das Glas stabilisiert wird. Dieser Grenzwert ist niedriger für das zweidimensionale System.

Für das dipolare System existiert eine experimentelle Realisierung von König et al. mit dem die Ergebnisse verglichen werden können. Es ergibt sich eine gute Übereinstimmung für das Plateau-Schermodul. Der kritische Parameter Γ_c zeigt eine von MCT-Rechnungen bereits für andere Systeme bekannte Abweichung um den Faktor zwei.

Eine Störungsrechnung, bei der das Schermodul als Summe der Schermoduln der einzelnen Komponenten der Mischung berechnet wird, zeigt eine gute qualitative und teilweise sogar quantitative Übereinstimmung mit der zwei-Komponenten Rechnung. Allerdings wird das Maximum der Kurve in der Region mit vielen sehr kleinen Kugel überbewertet.

Insgesamt scheint die Modenkopplungstheorie bei den untersuchten Systemen in den betrachteten Bereichen gute Ergebnisse zu liefern. Nur bei sehr kleinen Mischungsverhältnissen sieht man Abweichungen der Störungslösung von der anderen. Dies liegt vermutlich an beginnender Kristallbildung.

Abstract

In this thesis a Mode Coupling Theory (MCT) equation is derived that calculates the shear modulus for multi-component colloidal mixtures in two-dimensional systems in linear approximation.

With this equation, the plateau shear modulus G_∞ is calculated for two two-dimensional systems at the glass transition: for a binary mixture of hard spheres and for a binary mixture of dipolar particles.

The results for the shear modulus are compared with a three-dimensional system of hard spheres using data by Götze and Voigtmann. The plateau shear modulus has about the size $\frac{G_\infty}{nk_B T} \approx 20$ and a variation of ± 10 for all systems. Here n denotes the total number density.

We find that for all systems (the dipolar, the two-dimensional and the three-dimensional hard sphere system) the critical surface (ϕ_c resp. Γ_c) and G_∞ have maxima in the region of large differences in the size of the particles and large concentration of the smaller particles. We disagree with the common explanation of depletion attraction for this effect but show that the maxima in the plateau shear modulus are produced by the big particles and the force of the small ones on them.

With exception of the region of these maxima, all systems show a lowering of G_∞ through mixing. This can be compared to the effect of plasticizing for polymers.

The glass transition surface shows that for all systems the liquid is stabilized, but for the hard sphere systems there exists a threshold for the size ratio of the particles. Above that the glass is stabilized. This threshold is lower for the two-dimensional system.

For the dipolar system there exist experimental values for the system developed by König et al. A comparison shows a good agreement of the plateau shear modulus. The transition parameter Γ_c is overestimated by MCT by a factor two, as has been found for other systems.

A perturbational method, where the shear moduli of the particles are calculated separately as would be done for a monodisperse system and then added up, shows good qualitative and mostly even quantitative agreements with the two-component calculation, although the maximum in the region of large differences in the size of the particles and large concentration of the smaller particles is overestimated.

Overall MCT seems to yield good results for the systems studied here. Only close to the boundaries some small-scale crystallizing is visible in the particle plots of the dipolar system.

Contents

1. Introduction	1
2. Concepts and definitions	3
2.1. Colloids	3
2.2. Glass transition	3
2.3. Mode Coupling Theory	4
2.3.1. Derivation	4
2.3.2. Two-component system	5
2.4. Viscoelasticity	6
2.4.1. Viscosity	6
2.4.2. Elasticity	6
2.4.3. Stress relaxation modulus	7
2.4.4. Maxwell Model	8
2.4.5. Sinusoidal Strain	8
3. Shear modulus in two dimensions	9
3.1. Shear modulus with MCT	9
3.2. Derivation for two-dimensional systems	9
3.3. Normalization of the shear modulus	11
3.4. Normalization of the correlator	11
3.5. Monodisperse system	12
3.6. Perturbation of a one-component system	13
3.7. Model systems	13
3.7.1. Program	13
4. Glass transition of hard spheres	15
4.1. System	15
4.2. Shear modulus	18
4.3. Summary	19
5. Glass transition of dipolar particles	21
5.1. System	21
5.2. Shear modulus	24
5.3. Comparison with experiment	25
5.4. Summary	26
6. Interpretation of the results	27
6.1. Perturbation of a mono-disperse system	27
6.2. Smurfy region	29
7. Conclusion	31
A. Additional Figures in 3D rendering	33
Bibliography	37

1. Introduction

Whenever you want to put some ketchup on your fries, you have to shake the ketchup bottle. Otherwise it will be stuck inside.

This is just one of many examples that show, how the rheology – the way something flows – of highly viscous materials affects our lives. It also is a relatively new and fast developing part of science. Two topics in the example above are of importance for this thesis:

For one thing, we are looking at materials at the glass transition. The glass transition is characterized through a diverging of the relaxation times. This is the time the particles in the material need to reach their equilibrium state after the system has been disturbed. (This can be seen for ketchup, though it is not a glass: When the bottle is turned upside down, it needs a long time to flow down.)

The first microscopic approach to predict glass transition phenomena is the Mode Coupling Theory (MCT). It was developed in 1984 by Bengtzelius, Götze and Sjölander [1] and studied in detail by Götze [2]. It uses a density correlator formalism.

The simplest system that shows a glass transition is a colloidal system of hard spheres. A Colloid is a liquid with solid spheres in it that are so small that they show Brownian motion because of the liquid. This system is experimentally easy to control and to observe with optical microscopes. MCT has been tested there by Franosch et al.[3] and found to give good results.

Since it is an easy model system for the glass transition, it has also been used to study how the spatial dimension d changes the glass transition for higher dimensions by Schmid and Schilling [4] and for $d = 2$ by Bayer et al.[5].

But monodisperse systems tend to crystallize instead of forming a glass. Therefore, and because mixing phenomena are relevant in real life, it is interesting to study a binary mixture of hard spheres. This has been done in three dimensions by Götze and Voigtmann [6] and in two dimensions by Hajnal [7]. For another simple two-dimensional system, a binary mixture of dipolar particles, there exists an experimental setup by König et al. [8].

The other property of ketchup mentioned above which we are interested in is the rheology. Here we will concentrate on shear (see the figure on the title page¹), because that is experimentally and theoretically easily accessible. When a liquid is sheared, its flow can be described by the Newtonian viscosity η_0 . A solid body, however, responds elastically like a spring with a (constant) shear modulus G . A viscoelastic material combines those two responses. It can exhibit many effects. For example when it is sheared for a long time, the shear modulus $G(t)$ is high at first, then drops to a limiting value G_∞ because the material flows to compensate the pressure. When viscoelastic materials are studied, it is easiest to use viscoelastic fluids, because they perform Brownian motion. So they move randomly about and thus are able to explore their phase space while granular media like sand would have to be shaken.

¹The original version of the figure on the title page has been taken from <http://theorie.physik.uni-konstanz.de/lmfuchs/research.html>.

It is an interesting topic how mixing changes the shear modulus. For this, a formula for $G(t)$ in the linear regime has been derived by Nägele and Bergenholtz [9]. They use an MCT-approximation and express the shear modulus in terms of the density correlators. With this formula Götze and Voigtmann [6] have calculated the plateau shear modulus G_∞ in three dimensions for the model system of hard spheres.

Here we will adapt the formula for two-dimensional systems and with it calculate the plateau shear modulus of the two two-dimensional binary systems of hard spheres (or disks) and dipolar particles at the glass transition. Along with that we will combine the two topics introduced above. Thus we will see if the rheological properties of our simple model systems at the glass transition change for two dimensions, and – by comparing to experimental data – how good our results are.

First the needed formulas and main concepts shall be introduced, then we will derive an MCT-formula for the shear modulus in linear approximation. We will look at the two model systems separately, then compare them and try to find some explanations for the effects found. Additional three-dimensional figures will be found in the Appendix.

2. Concepts and definitions

In this section the concepts and formulas needed for this work will be introduced. Thereby only necessary topics will be discussed.

2.1. Colloids

Technically, a colloid is a component mixed in another one so that the component does not dissolve but forms a rigid structure on a scale of nano- to micrometers. Examples are foams, gels and emulsions. Here the term is used for solid, isotropic spheres of aforesaid size in a liquid. The spheres are thus so small that they perform Brownian motion because of the liquid. A simple system for testing soft matter theories is a liquid with hard spheres with a size below some micrometers.

The behavior of the system can usually be characterized by only a few static parameters, like the diameter of the particles, the number density and how they interact. But while these parameters describe the system accurately, dynamic quantities cannot be calculated with them.

2.2. Glass transition

Some systems have a state that behaves like something between a liquid and a solid and is called the glassy state. This is not a separate phase in the thermodynamical sense, because there are no phase transition singularities in the thermodynamic parameters. The structure of the glass is not distinguishable from liquid state without considering dynamical quantities like the mean square displacement.

For measurements in experiments often a threshold of viscosity of 10^{12}Pa is used as a definition.

From the theoretical point of view the ideal glass transition is the point where the system becomes non-ergodic without crystallizing. An ergodic system can explore the whole phase space over time, whereas a non-ergodic system is 'stuck' in a region. This can happen because the particles are so densely packed that they are encaged by each other. This also explains that the shear modulus G_∞ is non-zero in a glass, but zero in a liquid: In a glass, the particles cannot reorganize freely to adopt to the shear. It also validates the experimental threshold (which nevertheless stays arbitrary), because the viscosity of a glass would diverge in theory. In reality, however, there are other processes which hinder this. For example hopping processes, where a particle leaves its cage, are ignored by the theories used to describe the glass transition, as by MCT in the next section.

2.3. Mode Coupling Theory

The Mode Coupling Theory (MCT) is a theory to describe liquids as well as the glass transition and glassy processes.

2.3.1. Derivation

We will give a review of the central formulas and their derivation for an isotropic monodisperse (=one-component) system with spherically symmetric colloidal particles, where the particles perform Brownian motion on the basis of [10] and [11].

A microscopic analysis of the movements of Brownian particles in terms of the Fourier transformed distribution function n_k

$$n_k(t) = \sum_{i=1}^N e^{i\vec{k}\vec{r}_i(t)}$$

yields the Smoluchowski equation

$$\partial_t n_k(t) = \Omega^\dagger n_k(t)$$

with the adjoint Smoluchowski operator

$$\Omega^\dagger = \sum_i (\vec{\partial}_i + \vec{F}_i) \cdot \vec{\partial}_i$$

The sum is over all particles. $\vec{F}_i = -\partial_i \mathcal{U}(\{\vec{r}_i\})$ is the internal force on one particle for the total interaction potential \mathcal{U} .

A simple quantity for describing glassy phenomena is the density correlation function

$$\Phi_k(t) = \left\langle \frac{1}{N} n_k^*(t) n_k(0) \right\rangle_{TL}$$

$\langle \dots \rangle_{TL}$ means averaging in the thermodynamic limit. Φ has the limits $S_k = \Phi_k(0)$, which is called the static structure factor, and the nonergodicity parameter $F_k = \Phi_k(t \rightarrow \infty)$, which is zero if the system is ergodic.

By projecting the time-evolution solution of the Smoluchowski equation

$$n_k(t) = e^{\Omega^\dagger t} n_k(0)$$

onto a reduced and an irreducible part, using the uniqueness of the solution of a differential equation and consider this in terms of the correlator Φ , we get a Zwanzig-Mori equation

$$\partial_t \Phi_k(t) + \Gamma_k(t) \left\{ \Phi_k(t) + \int_0^t dt' m_k(t-t') \partial_{t'} \Phi_k(t') \right\} = 0$$

This formula is exact, but it can only be evaluated with an approximation of the memory function m , which is a four-point correlation function. $\Gamma_q(t) = D_0 q^2(t) / S_q(t)$ is the initial decay rate.

The mode coupling theory approximates the memory function m as a product of two-point correlation functions. This yields

$$m_q(t) = \frac{1}{2N} \sum_k \frac{S_q S_k S_p}{q^4} V_{\vec{q}\vec{k}\vec{p}} V_{\vec{q}\vec{k}\vec{p}} \Phi_k(t) \Phi_p(t)$$

with the vertex functions

$$V_{\vec{q}\vec{k}\vec{p}} = \vec{q} \cdot (\vec{k} n c_k + \vec{p} n c_p) \delta_{\vec{q}, \vec{k} + \vec{p}}$$

where the equation for $m_k(t)$ is seen as a bilinear functional \mathcal{F} of the correlation function Φ .

The direct correlation function c_k is given by the Ornstein-Zernike relation

$$S_k = 1/(1 - n c_k)$$

By using the Zwanzig-Mori equation with the approximation for $m_k(t)$, we get a fix-point relation for F_k

$$F_k = S_k - \{S_k^{-1} + \mathcal{F}(F_k, F_k)\}^{-1}$$

Since F changes at the glass transition because there the system becomes non-ergodic, it is possible to calculate the glass transition with the MCT equations.

For this, the static structure factor S is needed as an input. It can be calculated with Monte-Carlo methods, the Percus-Yevick method or with the hypernetted chain approximation (HNC).

2.3.2. Two-component system

The derivation presented here is for a one-component system, but except for mathematical differences nothing changes for an m -component system. We will present here the adapted definitions that will be used throughout the text. The particles will be counted by $\alpha, \beta \in 1, \dots, m$ with numbers of particles N_α , $N = \sum_\alpha N_\alpha$, relative number densities $x_\alpha = \frac{N_\alpha}{N}$ of the components and with the number density $n = N/V$.

$$\Phi^{\alpha\beta}(k, t) = \left\langle \frac{1}{N} n_k^{\alpha*}(t) n_k^\beta(0) \right\rangle_{TL}$$

with

$$n_k^\alpha(t) = \sum_{i=1}^{N_\alpha} e^{i\vec{k}\vec{r}_i(t)}$$

The static structure factor $S(k)$ is defined as $S(k) = \Phi(k, 0)$ and the nonergodicity parameter $F(k)$, which is zero if the system is ergodic, as $F(k) = \Phi(k, t \rightarrow \infty)$. This definition gives $\lim_{k \rightarrow \infty} S^{\alpha\beta}(k) = x_\alpha \delta_{\alpha\beta}$. The normalization can be chosen differently, cf. 3.4. The matrix Φ is a symmetric $m \times m$ -matrix, and thus also S and F .

A normalized direct correlation function $C_{\alpha\beta} = \sqrt{n_\alpha n_\beta} c_{\alpha\beta}$ can be defined for an m -component system by the Ornstein Zernike relation with 1 as identity

$$S(1 - C) = 1$$

The correlation function Φ can be decomposed as

$$\Phi^{\alpha\beta}(k, t) = x_\alpha \delta_{\alpha\beta} \Phi_\alpha^s(k, t) + x_\alpha x_\beta \Psi^{\alpha\beta}(k, t)$$

with the self-correlator

$$\Phi_\alpha^s(k, t) = \langle e^{-i\vec{k}(\vec{r}_{\alpha i}(t) - \vec{r}_{\alpha i}(0))} \rangle_{TL}$$

and a remainder $\Psi^{\alpha\beta}$. Here $\vec{r}_{\alpha i}(t)$ denotes the position of particle i of sort α at time t .

2.4. Viscoelasticity

For understanding what is presented in this thesis, it is good to look a bit deeper into the theory of viscoelastic materials without the correlator notation, because this makes it easier to connect the results to real life.

In this text, we look at linear viscoelasticity only. This is with very small shearing, so that no difficult effects like turbulence can appear. For a figure of shear please look at the title page.

2.4.1. Viscosity

As in the hands-on description of the shear viscosity η in the introduction, it can be defined as the ratio of shear stress (this is force per area or in two dimensions force per length) versus shear strain rate (gradient of the velocity of the liquid):

$$\sigma = \eta \dot{\gamma}$$

where σ is the shear stress and $\dot{\gamma}$ the velocity gradient (or, in linear regime, the shear rate). While η is constant for Newtonian fluids, it usually depends on the shear rate.

2.4.2. Elasticity

The most simple form of elasticity is when the shear stress σ of a solid body is proportional to the shear strain (the gradient of the displacement) γ with the elasticity E as the proportionality constant.

$$\sigma = E\gamma$$

Because a hard body can be deformed in several ways and directions, E usually is a tensor.

Often the elastic modulus depends on time and on the history of the material. We will only present the theory of linear elasticity of viscoelastic materials for one-dimensional stress and shear, following [12]. When the strain is controlled, the stress at time t can be written as a functional \mathcal{A} that depends on the strain at all times before and on the time t

$$\sigma = \mathcal{A}[\gamma(s)|_{s=-\infty}^t, t]$$

The response is called linear, if scaling and superposition of two strain histories γ_1 and γ_2

$$\gamma(s) = \lambda_1 \gamma_1(s) + \lambda_2 \gamma_2(s)$$

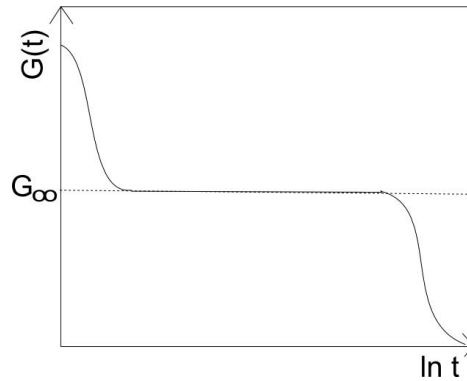


Figure 2.1.: Shear stress relaxation modulus in a glass. For small times, it decreases towards G_∞ . Then it stays constant for a long time, because the material is nonergodic and so cannot reorganize itself to compensate the stress. It has been observed in experiments that for very long times the shear modulus drops towards zero because of hopping processes. In an ideal glass this would not be the case.

with $\sigma_i = \mathcal{A}[\gamma_i(s)|_{s=-\infty}^t, t]$ result in

$$\sigma(s) = \lambda_1 \sigma_1(s) + \lambda_2 \sigma_2(s)$$

This does not mean that the response curve of the material looks linear.

If the material does not age, the functional only depends on the time-difference: $\sigma = \mathcal{A}[\gamma(t-s)|_{s=0}^\infty]$.

2.4.3. Stress relaxation modulus

When an elastic material is deformed and kept this way for a long time, the stress usually does not stay constant. It starts at a high value, then decreases and finally reaches a constant value (often non-zero). This is called stress relaxation. The reason for this is that the particles of the material reorganize themselves to adapt to the deformation. But since some materials like glasses are nonergodic, they cannot freely change shape thus that a residual stress remains.

For a step-strain history where the strain can be described by a Heaviside-function, $\gamma(s) = \gamma_0 H(t)$, the response is (due to linearity)

$$\sigma(t) = \gamma_0 \mathcal{A}[H(t-s)|_{s=0}^\infty] =: \gamma_0 G(t)$$

$G(t)$ is the elastic stress modulus. It is reasonable that $G(t)$ is greater than zero and for nonergodic materials decays to a non-negative limit G_∞ for $t \rightarrow \infty$. In fig.2.1 an example for $G(t)$ in a glass is given.

As all changes in strain can be described by Heaviside functions (similar to the step function in integration theory), a Stiltjes integral for non-aging linear materials can be derived

$$\sigma(t) = \int_{s=0}^t G(t-s) d\gamma(s)$$

For differentiable variables this can be written as

$$\sigma(t) = \gamma(0)G(t) + \int_{s=0}^t G(t-s) \frac{d\gamma(s)}{ds} ds$$

2.4.4. Maxwell Model

The Maxwell Model was invented to describe viscoelastic solids. It combines the reactions of solids – stress is linear to strain –, with the reactions of liquids, where stress is linear to strain rate.

$$\sigma = \eta \dot{\gamma} + G\gamma$$

For a step-strain, the solution is

$$G(t) = G_{\infty} + (G(0) - G_{\infty})e^{-t/\tau_R} = G_{\infty} + \Delta G(t)$$

where τ_R is the characteristic stress relaxation time.

2.4.5. Sinusoidal Strain

For a small sinusoidal strain ($\omega \ll 1$)

$$\gamma(t) = \gamma_0 \sin(\omega t)$$

the stress oscillates after a settling time with

$$\sigma(t) = \gamma_0(G'(\omega) \sin(\omega t) + G''(\omega) \cos(\omega t))$$

G' and G'' are called storage and loss modulus and are related to $G(t)$ by

$$G'(\omega) = G_{\infty} + \omega \int_{s=0}^{\infty} \Delta G(s) \sin(\omega s) ds$$

$$G''(\omega) = \omega \int_{s=0}^{\infty} \Delta G(s) \cos(\omega s) ds$$

For $\omega \rightarrow 0$, the stress converges to $\sigma(t) = \gamma_0 G_{\infty}$.

In the following we will use $\gamma_0 \rightarrow 0$ to be in the linear regime, and $\omega \rightarrow 0$ to determine G_{∞} .

3. Shear modulus in two dimensions

3.1. Shear modulus with MCT

In [9] Bergholtz and Nägele give a complete derivation of $G(t)$ for m -component mixtures in terms of the correlators for three dimensional systems. They define the shear stress σ_{xy}

$$\sigma_{xy} = - \sum_i F_i^\alpha r_i^\beta$$

via the action of the Smoluchowsky equation under flow on the equilibrium distribution function

$$\begin{aligned} \Omega &= \Omega_e + \delta\Omega \\ \delta\Omega &= -j \sum_i \frac{\partial}{\partial x_i} y_i \end{aligned}$$

Now the potential part of the stress tensor is written in the zero wave-vector limit. This leads to the result that the shear relaxation function is the shear stress autocorrelation function.

$$G(t) = \frac{1}{k_B T V} \langle \sigma_{xy}(0) e^{t\Omega^\dagger} \sigma_{xy}(0) \rangle = \frac{1}{k_B T V} \langle \sigma_{xy}(t) \sigma_{xy}(0) \rangle$$

The viscosity is given by a Green-Kubo formula as

$$\eta = \int_0^\infty G(t) dt$$

The MCT approximation is made. Bergholtz and Nägele project the solution onto the slow variables, which is the particle density. As in 2.3 the four-point correlation functions are approximated as two-point correlation functions. The sum over k that comes from the projection is written as an integral. Because of the shear the potential part of $U = e^{\Omega^\dagger t}$ is $U_{\alpha\beta}^p(k) = \frac{k_x k_y}{k} k_B T \frac{d}{dk} S_{\alpha\beta}(k)$. Hydrodynamic actions, which would give another term for U , are ignored.

Using the Ornstein-Zernike equation and transforming the integral over \vec{k} to an integral over k yields a three-dimensional MCT equation for the shear relaxation modulus.

$$G(t) = \frac{k_B T}{60\pi^2} \int_0^\infty k^4 \cdot \text{Tr} \left[\left(\frac{dC(k)}{dk} \Phi(k, t) \right)^2 \right] dk$$

3.2. Derivation for two-dimensional systems

The derivation of a formula to calculate the shear modulus $G(t)$ from the structure factors $S(k) = \Phi(k, 0)$ and $S(k, t)$ in two dimensions is done analogously to the derivation in three

dimensions in [9]. All numbers of equations in this section relate to the three-dimensional derivation. $S(k)$ is defined differently in [9] than in 2.3. However, we will show that the result is the same in 3.4. All involved matrices are symmetric.

Since this is easy to do, we will give the formula for a d -dimensional system (with $d > 1$). For this, only a few adaptations of the derivation are necessary since the more abstract parts are independent of dimension.

The equations in [9] relevant for the dimension are (61), where a sum over k is replaced by an integral $V/(2\pi)^3 \int d\vec{k}$, (62) and (63) together with (68), which gives a factor $\left(k_B T \frac{k_x k_y}{k}\right)^2$ in the integral, and (72), where a transformation from $\int d\vec{k}$ to $\int dk$ is made. The strain rate tensor in (2) depends on the dimension as well.

The changes in the formula for a d -dimensional system shall now be discussed with reference to the number of the equation at which they appear in [9].

- (2) The entries of the strain rate tensor are defined by $(E_0)_{ij} = \frac{1}{2}(\frac{\partial u_i}{\partial x_j} + \frac{\partial u_j}{\partial x_i})$, where $\vec{u}(\vec{x})$ is the velocity profile. For shear, only two symmetric entries are not zero.

In two dimensions this is simply

$$E_0 = \frac{\dot{\gamma}}{2} \begin{pmatrix} 0 & 1 \\ 1 & 0 \end{pmatrix}$$

For higher dimensions, the rest of the matrix has to be filled with zeros in all other places. (Where in the matrix the non-zero entries are, depends on the definition of the coordinates.)

- (57) to (61) The sum over \vec{k} can be written as an integral $V/(2\pi)^d \int d\vec{k}$, where V is a (d -dimensional) volume in k -space. Since (57) has a term $1/V$ (stemming from equation (12)) the V cancels out.

- (68) As U^p depends on E_0 , this explains that it always has the same form as in three dimensions. So we get a factor $\left(k_B T \frac{k_x k_y}{k}\right)^2$ in the integral. The rest of the integral only depends on $k = |\vec{k}|$.

- (72) We get a factor $\oint d\Omega_k \left(\frac{k_x k_y}{k}\right)^2$ that is different for each dimension. For three dimensions we get $\frac{4\pi}{15} k^4$, while in two dimensions

$$\oint d\Omega_k \left(\frac{k_x k_y}{k}\right)^2 = \frac{k^5}{k^2} \int_0^{2\pi} \cos^2 \varphi \sin^2 \varphi d\varphi = \frac{\pi}{4} k^3$$

All put together we get for the d -dimensional system

$$G(t) = \frac{k_B T}{2} \frac{1}{(2\pi)^d} \int_0^\infty \oint \left(\frac{k_x k_y}{k}\right)^2 d\Omega_k \text{Tr} \left[\left(\frac{dC(k)}{dk} \Phi(k, t) \right)^2 \right] dk$$

and for $d = 2$

$$G(t) = \frac{k_B T}{32\pi} \int_0^\infty k^3 \text{Tr} \left[\left(\frac{dC(k)}{dk} \Phi(k, t) \right)^2 \right] dk$$

with $t \rightarrow \infty$, $\lim_{t \rightarrow \infty} \Phi(k, t) = F(k)$

$$G_\infty = \frac{k_B T}{32\pi} \int_0^\infty k^3 \text{Tr} \left[\left(\frac{dC(k)}{dk} F(k) \right)^2 \right] dk \quad (3.1)$$

Now we will introduce the notation for the two-dimensional system. As the 2×2 -matrices are symmetric we can write

$$S(k) = \begin{pmatrix} S_0 & S_1 \\ S_1 & S_2 \end{pmatrix}$$

The matrix-operations can be given explicitly, since this is still possible for 2×2 matrices. The Ornstein-Zernike relation yields for the two-component system

$$\begin{aligned} C_0 &= C_{bb} = 1 - \frac{S_2}{S_0 S_2 - S_1^2} \\ C_1 &= C_{bs} = \frac{S_1}{S_0 S_2 - S_1^2} \\ C_2 &= C_{ss} = 1 - \frac{S_0}{S_0 S_2 - S_1^2} \end{aligned}$$

and with $C' = \frac{dC}{dk}$ the Trace is

$$\begin{aligned} \text{Tr} &= \text{Tr} \left[\left(\frac{dC(k)}{dk} F(k) \right)^2 \right] \\ &= C_0'^2 F_0^2 + 2C_0' F_1 (2C_1' F_0 + C_2' F_1) + 4C_1' C_2' F_1 F_2 + C_2'^2 F_2^2 + 2C_1'^2 (F_1^2 + F_0 F_2) \end{aligned}$$

3.3. Normalization of the shear modulus

Since we want to study mixing effects and not the changes that come from varying the parameters of a one-component system, we will give the shear modulus as $G_\infty / (nk_B T)$. By this, the limit of the one-component system will be constant.

3.4. Normalization of the correlator

The density correlator $\Phi(k, t)$ can be calculated with different normalizations. For the derivation in 3.2 $S(k)$ is defined in such a way that the diagonal values of $S(k)$ go to one for large k . Often, however, the data is defined as in 2.3 so that for large k the diagonal values converge to the concentration of the component.

In [9], which was used for the derivation of G_∞ , the following definition was introduced in equation (56)

$$S_{\alpha\beta} = \langle A_k^\alpha A_{-k}^\beta \rangle$$

with

$$\begin{aligned} A_k^\alpha &= \frac{1}{\sqrt{N_\alpha}} \sum_{l=1}^{N_\alpha} e^{-i\vec{k}\vec{R}_l^\alpha} - \sqrt{N_\alpha} \delta_{\vec{k},0} \\ &= \frac{1}{\sqrt{N_\alpha}} n_k^\alpha - \sqrt{N_\alpha} \delta_{\vec{k},0} \end{aligned}$$

n_k^α is defined as in 2.3.2. For $k \neq 0$ this can be transformed to the definition of $S(k)$ in 2.3.2, which will here be called $S'_{\alpha\beta}$.

The case $k = 0$ can be ignored here, as S is non-continuous but finite there because of the definition and only $k \cdot S$ appears in the formula for the shear modulus, which is zero for $k = 0$.

$$\begin{aligned} S_{\alpha\beta}(k) &= \left\langle \frac{1}{\sqrt{N_\alpha N_\beta}} n_\alpha n_\beta \right\rangle \\ &= \frac{N}{\sqrt{N_\alpha N_\beta}} S'_{\alpha\beta}(k) \\ &= \frac{1}{\sqrt{x_\alpha x_\beta}} S'_{\alpha\beta}(k) \end{aligned}$$

The same relation is valid for $F(k)$.

However, it can be shown in a straightforward calculation that for transformations of that kind (with symmetric 2×2 matrices and arbitrary, not k -dependent x_α, x_β), the trace of $(\frac{dC}{dk} F)^2$ stays the same, because all x_α and x_β cancel out. The shear modulus also is the same if a concentration-dependent Ornstein-Zernike relation is used as often found in other sources.

That is the reason why the shear modulus does not depend on the normalization of the correlation functions, as long as it is the same for S and F .

3.5. Monodisperse system

A one-component system with N particles and the correlator $\Phi(k, t)$ can be seen as a mixture of two components of the same size with $N = N_\alpha + N_\beta$, $x_\alpha = N_\alpha/N$. This allows a test of the derived two-component formula, because the plateau shear modulus can be calculated with the one-component and with the two-component formula. Both results should then be the same. Here we will derive the two-component structure factor for the system. First we will split the monodisperse correlator into the entries of the two-component correlator. For the definitions see 2.3.2.

$$\begin{aligned} \Phi(k, t) &= \left\langle \frac{1}{N} \sum_{i=1}^N e^{-ikr_i(t)} \sum_{j=1}^N e^{jkr_j(0)} \right\rangle \\ &= \left\langle \frac{1}{N} n^*(t) n(0) \right\rangle \\ &= \left\langle \frac{1}{N} (n_\alpha(t) + n_\beta(t))^* (n_\alpha(0) + n_\beta(0)) \right\rangle \\ &= \left\langle \frac{1}{N} n_\alpha^*(t) n_\alpha(0) \right\rangle + \left\langle \frac{1}{N} n_\beta^*(t) n_\beta(0) \right\rangle + \left\langle \frac{1}{N} n_\alpha^*(t) n_\beta(0) \right\rangle + \left\langle \frac{1}{N} n_\beta^*(t) n_\alpha(0) \right\rangle \\ &= \Phi_{\alpha\alpha}(k, t) + \Phi_{\alpha\beta}(k, t) + \Phi_{\beta\alpha}(k, t) + \Phi_{\beta\beta}(k, t) \end{aligned}$$

$\Phi_{\alpha\beta}(k, t)$ can be written as the sum of a self-correlated part and a remainder.

$$\Phi_{\alpha\beta}(k, t) = x_\alpha \delta_{\alpha\beta} \Phi_{\alpha\beta}^s(k, t) + x_\alpha x_\beta \Psi_{\alpha\beta}(k, t)$$

$\Phi(k, t)$ can also be written in this way $\Phi(k, t) = \Phi^s(k, t) + \Psi(k, t)$. As the particles behave the same whether we see them as two kinds or not, the average of the entries of the density correlator n has to be the same, only the number of summands is different. So we find $\Phi^s(k, t) = \Phi_{\alpha\alpha}^s(k, t)$ and $\Psi(k, t) = \Psi_{\alpha\beta}(k, t)$. It is obvious that $\Phi^s(k, 0) = 1$. Thus we get the two-component correlators which match the definition in 2.3.2.

$$\begin{aligned} S'_{\alpha\alpha} &= x_\alpha(1 + x_\alpha(S - 1)) \\ S'_{\alpha\beta} &= x_\alpha x_\beta(S - 1) \\ F'_{\alpha\alpha} &= x_\alpha(F^{self} + x_\alpha(F - F^{self})) \\ F'_{\alpha\beta} &= x_\alpha x_\beta(F - F^{self}) \end{aligned}$$

3.6. Perturbation of a one-component system

For large concentrations of one component, the other can be seen as a perturbation of a one-component system. For this only the diagonal entry of the majority component of the structure factors S and F has to be taken and the shear modulus can be calculated with the one-component formula:

$$\frac{G_{\infty\alpha\alpha}}{n x_\alpha k_B T} = \frac{1}{x_\alpha n} \frac{1}{32\pi} \int_0^\infty k^3 \left(\frac{1}{S_{\alpha\alpha}(k)} \frac{dS_{\alpha\alpha}(k)}{dk} \frac{F_{\alpha\alpha}(k)}{S_{\alpha\alpha}(k)} \right)^2 dk \quad (3.2)$$

By this, the other component is taken into account by the changes it makes in the structure factors. They could be represented as a potential between the majority particles.

3.7. Model systems

In the following chapters, the shear modulus shall be calculated for two two-dimensional model systems of binary mixtures: for a mixture of hard spheres with different sizes and for a mixture of dipolar particles with different susceptibilities.

3.7.1. Program

A program written by David Hajnal for his PhD thesis calculates coordinates and structure factors for binary mixtures of dipolar particles with a hard core with Monte-Carlo techniques and MCT. The dipolar interaction and the hard core radius can be set so that hard spheres and dipolar point particles can be simulated. As the program takes several weeks to run, Mr. Hajnal's already calculated data is used. It consists of several configurations of x_s and δ for mixtures at the glass transition for a hard sphere system and a system of dipolar point particles in two dimensions. Every data set of a simulation consists of the entries of the 2×2 matrices $S(k)$ and $F(k)$ for 250 discrete values of k , $k = 0.0606, 0.2606 \dots 50$.

These form the entry to my program, which calculates the plateau shear modulus $\frac{G_\infty}{n k_B T}$ for a model and saves the data for the different mixing configurations into a file. It is written in C++.

The program detects the number n_k of points in k -space, for which S and F are given and stores S and F into $n_k \times 3$ arrays, to use the symmetry of the matrices. S is transformed

into C using the Ornstein-Zernike relation. Then G_∞ is calculated using equation (3.1). The derivative and the integration are done by spline interpolation using the GSL (GNU Scientific Library). The result, as well as the configuration of the system and the critical parameter are written into a text-file.

A test of the program with structure data for hard spheres with diameter $d = 1$ given by Matthias Krüger gives the same result for the shear modulus as a calculation with the one component formula:

$$\frac{G_\infty}{k_B T / d^2} = 18.57$$

I have verified the results for the dipolar system with a Mathematica program developed by David Hajnal. An adaptation for three-dimensional systems also gives the same results as in [6].

4. Glass transition of hard spheres

4.1. System

In this chapter we will look at a binary mixture of hard spheres in two dimensions.

This system was studied by Weysser and Hajnal [13], [7] among others. It has been found that the two-dimensional MCT results are valid and similar to the results in three dimensions. For completeness, we will repeat parts of the analysis here.

Since we are interested in the way the spatial dimension changes the plateau shear modulus at the glass transition, it is fortunate that mixing and the plateau shear modulus was studied for the same system in three dimensions by Götze and Voigtmann [6]. We will thus be able to compare the systems.

The plots presented below are made with data calculated by the program of David Hajnal. He used a Monte-Carlo technique for the static structure factor S and calculated the nonergodicity parameter F in mode coupling approximation. For the definitions see 2.3.2. Because F is zero for a liquid and nonzero for a glass, he was able to determine the value of ϕ_c for a fixed set of x_s and δ at the glass transition with it. For more information about the calculations see [14].

The two-dimensional system consists of two kinds of hard spheres (or disks, since the system is two-dimensional), with radii R_s and R_b . Here s denotes the smaller and b the bigger particles, so that $R_s < R_b$. Since they are hard spheres they cannot overlap, but otherwise they do not interact. The interaction potential of a particle would thus be a delta-function of its radius $u_i(r) = \delta(r - r_i)$.

Since we want to study mixing phenomena, we will vary the relative number density x_s of the smaller particles and the size ratio $\delta = R_s/R_b$.

To study at the glass transition, we have to change the number density $n = N/V$ as well, otherwise the system would become more solid or more liquid.

By varying x_s and δ while keeping R_b constant, we change the packing fraction

$$\phi = n\pi R_b^2(x_b + x_s\delta^2)$$

This is a good indicator for how variations in the composition change the dynamics of the system. It can be seen as an inverse system temperature. If the packing fraction at the glass transition is low, then the particles will hinder/encage each other, although they would have enough space to move and the glass is stabilized. If the packing fraction at the glass transition is high, the particles are organized in a way that leaves them as much free space to move as possible and the liquid is stabilized.

In fig.4.1 four cuts through the critical surface (the values at the glass transition) of the packing fraction $\phi_c(\delta, x_s)$ are displayed. For small size disparities ($\delta > 0.5$), it can be seen that ϕ_c is reduced by mixing. Thus the glass is stabilized.

For small δ and high x_s , however, the critical surface has a maximum. Here the liquid is stabilized.

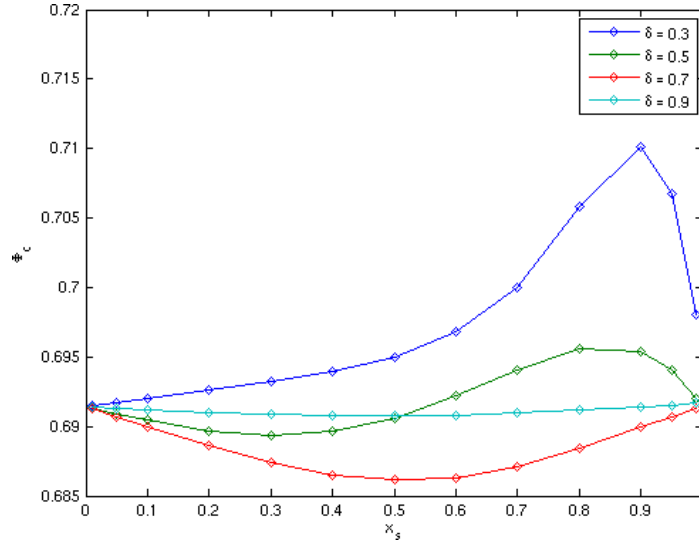


Figure 4.1.: Four cuts through the glass transition surface $\phi_c(x_s, \delta)$ for hard disks. For $\delta < 0.5$ the liquid and for $\delta > 0.5$ the glass is stabilized for mixing. ϕ_c has its maximum in the smurfy region (the region with many small particles).

As the region of small δ and high x_s where ϕ_c has its maximum shows many special phenomena that do not occur for higher δ or smaller x_s , it will be called the “smurfy edge”, as compared to the smurfs, where there is one big Gargamel and many small smurfs.

The critical surface is similar to the surface found for the three-dimensional system by Götze and Voigtmann, see fig.4.3 although the liquid-stabilizing regime starts in three dimensions at a higher size ratio $\delta < 0.7$. Here the concentration of small particles is given in terms of the relative concentration of small particles by volume $\hat{x}_s = \frac{\phi_s}{\phi}$. For the dimension d it is related to x_s via

$$x_s = \frac{\hat{x}_s / \delta^d}{1 + \hat{x}_s (1 / \delta^d - 1)}$$

MCT takes the static structure factor S of the system as only input. The glass transition and the plateau shear modulus, which we will look at later, are calculated with S and the nonergodicity parameters F . A closer look at these could be enlightening. Results, however, cannot be taken intuitively, because they are in k -space. k is given in terms of $\frac{1}{2R_b}$, but as R_b is left constant this can be ignored here.

The diagonal elements of the structure factors in figure 4.2 show the periodicity expected for hard spheres.

Let us consider S in the left column of fig.4.2. As a very weak effect, the maxima of S_{bb} seem to shift to higher k for higher x_s , while at the same time the height of the maxima decreases rapidly. For high δ ($\delta = 0.9$), the third panel S_{bb} is almost constant for large x_s . Even the minimum for very small k is almost gone.

The maxima of S_{ss} shift to lower k for lower x_s , and thus do not behave symmetrically. However, here we get the same effect that the maxima decrease rapidly when the relative concentration of the particles gets lower.

This decrease in S for the minority particles might mean that they are distributed ran-

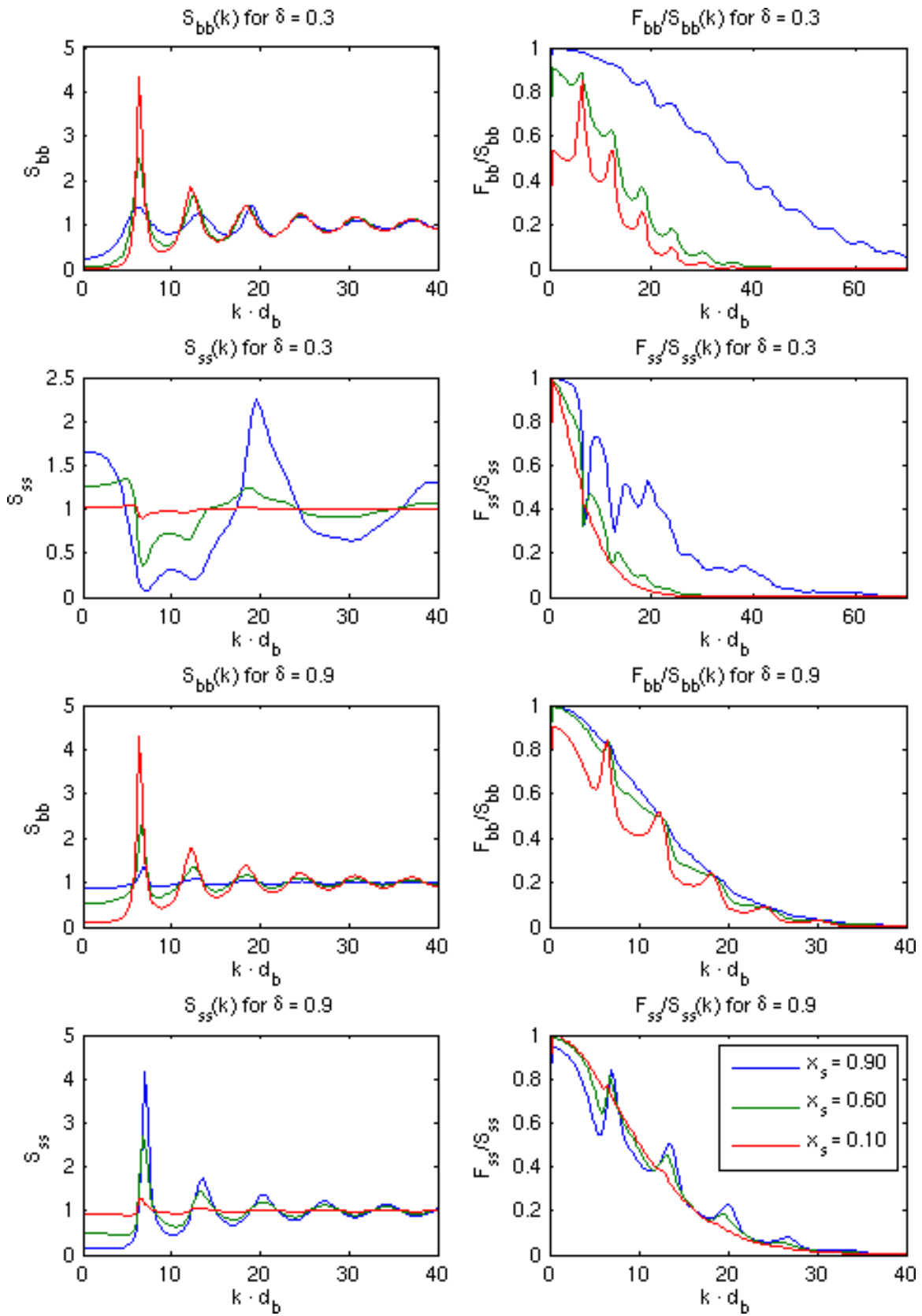


Figure 4.2.: Diagonal entries of $S(k)$ and $F(k)/S(k)$ for selected values of δ , x_s for the hard sphere system. The majority particles are strongly correlated.

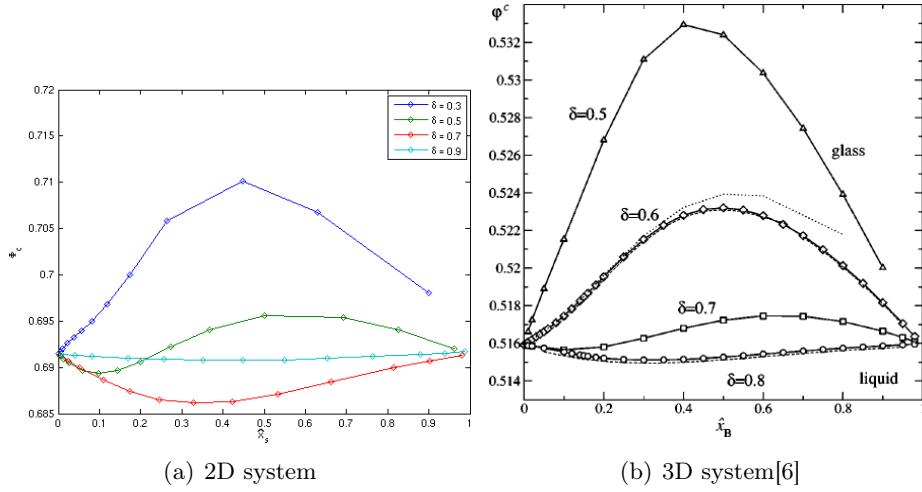


Figure 4.3.: Glass transition surface $\phi_c(\hat{x}_s)$ for the two- and three-dimensional system of hard spheres. The use of \hat{x}_s shifts the values of large x_s to the middle.

domly and are too far apart to “see” each other. Whether the high peaks and the periodicity in S of the majority particles indicate some crystallizing cannot be said. Nevertheless this is an important issue since it would render the MCT-calculations void, because MCT assumes homogeneity and isotropy. This topic will be discussed in 6.

The diagonal elements of the normalized nonergodicity parameter F/S in the right column in fig. 4.2 show the ideal curve in the upper panel: For large x_s , it is an approximation of a Gaussian, as one would get if just one particle is observed. In space-regime, the particle would diffuse, but because we are in a glass, it cannot. So where the particle can be, depends smoothly on the distance, because the particles around it are not organized. This is called the Lamb-Mößbauer factor.

For small x_s , F should be approximating the one-component limit. For intermediate x_s , the curves should smoothly interpolate between these two limits.

This behavior is the case for F_{bb} and at large δ also for F_{ss} . For small δ and large x_s – the smurfy region – however, F_{ss} differs from the behavior of the other curves. Also the near-Gaussian of F_{bb} is exceptionally wide in the upper panel. This can be seen as another indication that this region behaves differently.

4.2. Shear modulus

The plateau shear modulus $G_\infty/(nk_B T)$ is calculated on the critical surface $\phi_c(x_s, \delta)$ using equation (3.1). As input it uses the data for the two-dimensional system of a binary mixture of hard spheres calculated by David Hajnal [14] as discussed above with S and F at the glass transition for $x_s \in [0.01, 0.99]$ and $\delta \in [0.3, 0.9]$.

In figure 4.4 the plateau shear modulus is shown (as in all following figures) as $G_\infty/(nk_B T)$ so that the one-component value is the same at all boundaries.

It has been found for polymers that the addition of small particles in a system makes the

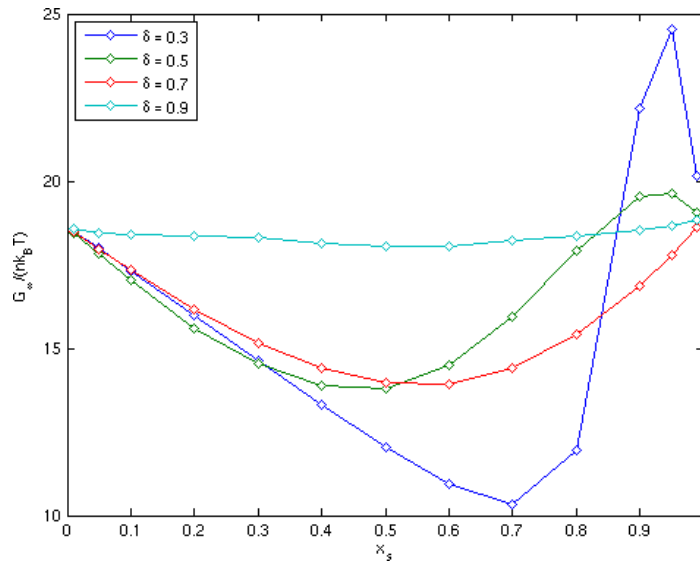


Figure 4.4.: Plateau shear modulus $G_\infty(x_s)$ for hard disks. Plasticizing is observed in the whole regime except for the smurfy region.

system “softer”. This is widely used to plasticize materials and make them more ductile. The term “plasticizing” is used there for this phenomenon and thus we will use the same term here.

The shear modulus shows plasticizing everywhere except in the smurfy region (with small δ and large x_s).

At the maximum of ϕ_c in the smurfy region the shear modulus increases for increasing x_s until it drops again to the constant boundary value. So putting a few big spheres in a system of small hard spheres while staying at the glass transition increases G_∞ .

These are qualitatively the same effects as for three dimensions, see fig. 4.5 and [6]. For large δ there is plasticizing as in the two dimensional system. In the smurfy region G_∞ seems to increase a bit above the boundary value for the three-dimensional system, while the two-dimensional system has a pronounced maximum of the shear modulus there before it drops again towards its boundary value. The height of the plateau modulus as well as its variation is about the same in both systems.

4.3. Summary

We have seen that the two-dimensional system behaves similar to the three-dimensional. When changing from three to two dimensions there seems to be a shift towards a stabilization of the glass. Φ_c decreases for $\delta > 0.5$ instead of $\delta > 0.7$. The peak of the plateau shear modulus of the two-dimensional system in the smurfy edge is a lot smaller in the three-dimensional system.

While the three-dimensional system has (except for very high δ) a shift through mixing towards the liquid for both ϕ_c and G_∞ , the two-dimensional system shows contradicting phenomena for $x_s < 0.8$ and $\delta > 0.5$: The solid is stabilized by mixing but plasticized,

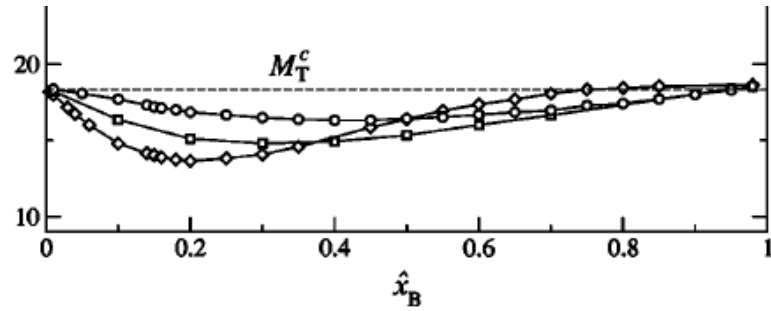


Figure 4.5.: Hard disks in 3D for comparison: G_∞ (here called M_T^c) plotted versus \hat{x}_s [6]. In fig. 4.3(a) and 4.1 can be seen how the values are shifted by the transformation between x_s and \hat{x}_s .

because the shear modulus decreases.

Our results mostly support the findings of Hajnal [7]. He showed that the mixing scenario in two dimensions is similar and shows the same effects as in three dimensions, while the extension of the glassy regime is more pronounced.

In this work however, differences can be seen for the smurfy region. While there seem to be no special phenomena in the smurfy region for the three-dimensional system, the two-dimensional inverts its behavior there: Suddenly the liquid is stabilized and the shear modulus increases.

5. Glass transition of dipolar particles

5.1. System

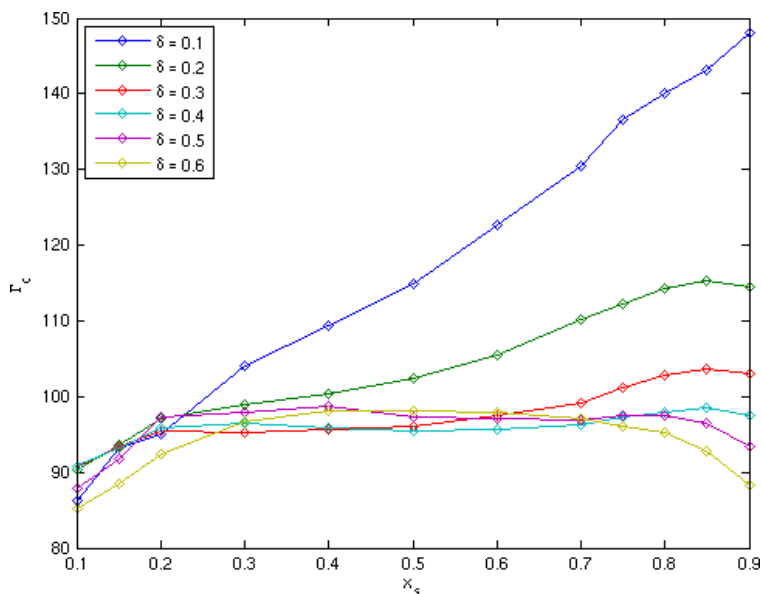


Figure 5.1.: Cuts through the glass transition surface $\Gamma_c(x_s, \delta)$ for the dipolar system. The glass is stabilized by mixing.

It is interesting to compare the calculations of the plateau shear modulus with the “real world”. So the second system that we study here is a simplified model of the system studied experimentally by König et al. [8]. They use super-paramagnetic colloidal particles at a two-dimensional water-air interface and induce a magnetic field so that they repel each other. The particles have mean distances of several radii of their hard cores, so we will ignore those. They interact via their dipole potential

$$u^{\alpha\beta}(r) = \frac{\mu_0 \chi_\alpha \chi_\beta B^2}{4\pi r^3}$$

Binary mixtures of this system have been studied theoretically in detail by David Hajnal [14]. The main parameters of the system are x_s , the concentration of small particles, and $\delta = \frac{\chi_s}{\chi_b}$, the ratio of the susceptibilities. The concentration n of all colloids is chosen as one. The dependence on T , n , B is given by the coupling parameter

$$\Gamma = (\pi n)^{3/2} \frac{\mu_0 [x_b + x_s \delta]^2 \chi_b^2 B^2}{4\pi k_B T}$$

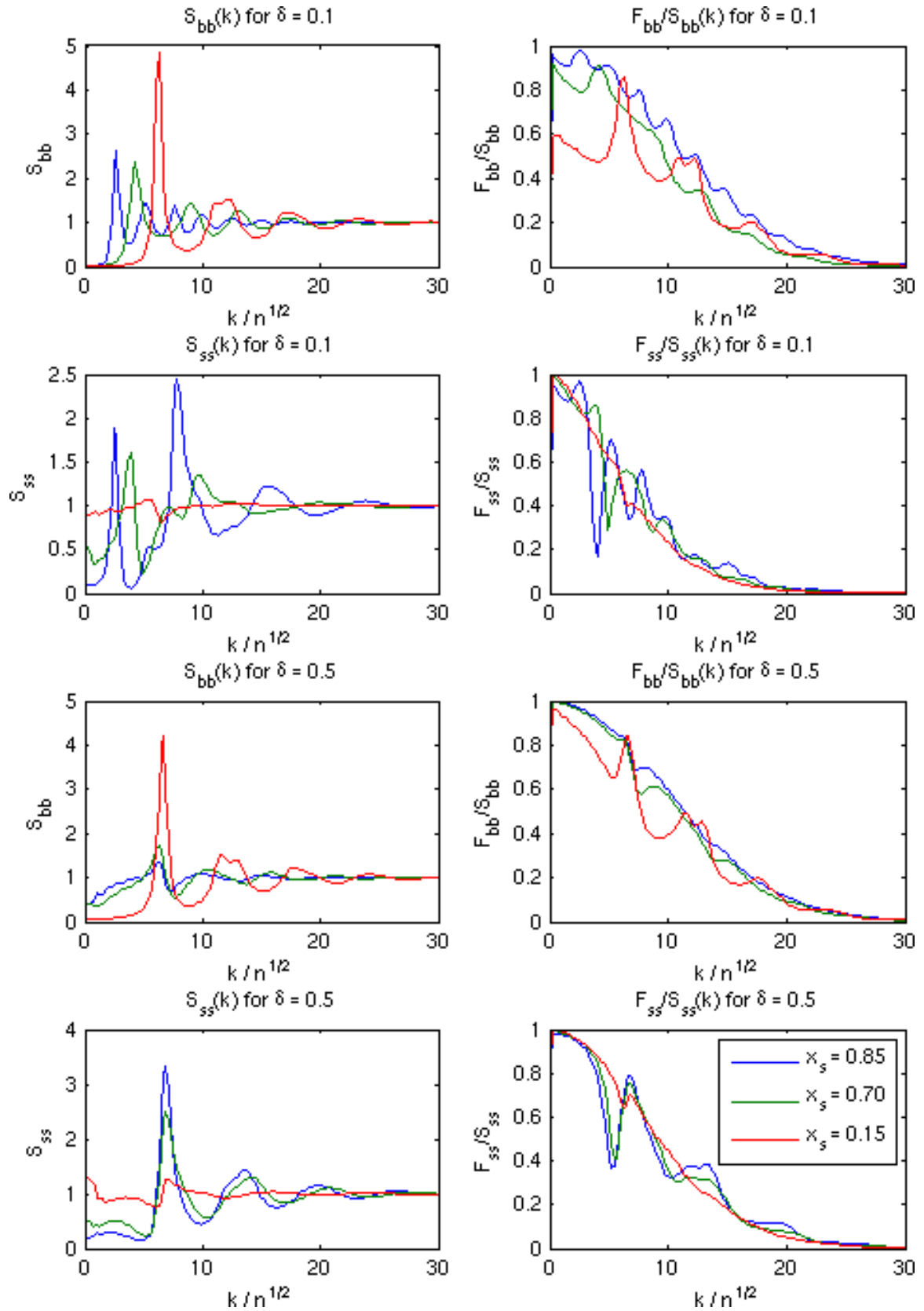


Figure 5.2.: Diagonal entries of $S(k)$ and $F(k)/S(k)$ for selected values of δ , x_s for the dipolar system. The correlation is stronger for the majority particle sort.

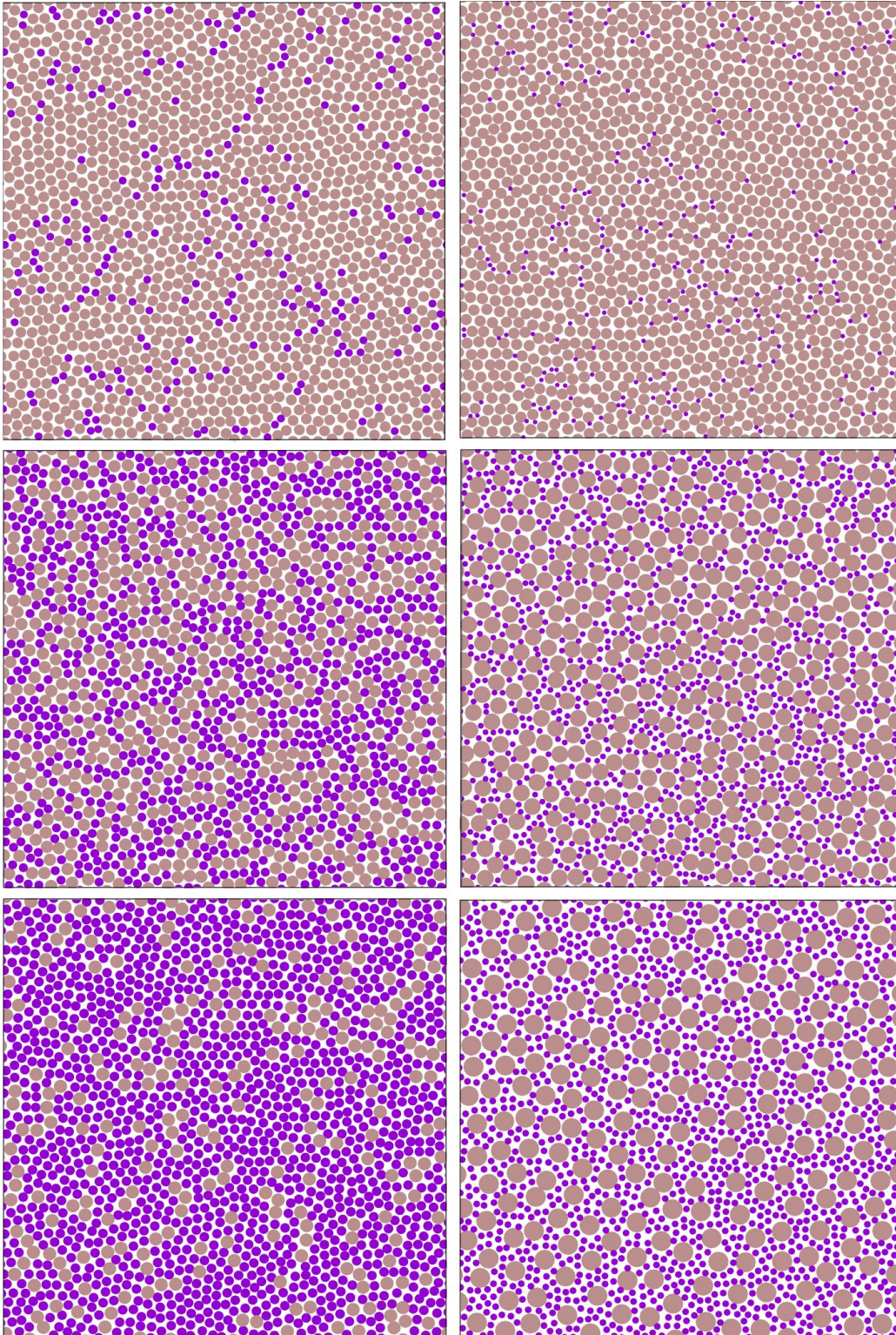


Figure 5.3.: Some configurations for dipolar particles with (left, top to bottom) $\delta = 0.5$, $x_s = 0.85, 0.6, 0.15$ and (right) $\delta = 0.1$, $x_s = 0.85, 0.7, 0.15$. The radii are just a guide to the eye, the ratio of radii is chosen as $\sqrt{\delta}$. For big and small x_s there seems to be some crystallizing on small scales except in the bottom left panel that shows the smurfy region.

The fact that the particles are presumed to be point particles leads to the following result. Different from the hard sphere system, the number density n does not need to be changed when the mixing parameters are chosen differently: The system can be brought to the glass transition by increasing the external magnetic field thus “pumping up” the particles.

The model system presented here has been proved as a practically correct means to describe the experimental system in terms of the structure factors. It has further been shown that MCT yields good results here.

The data used here has been calculated by Hajnal. Monte-Carlo techniques are used for the static structure factors. The glass transition surface $\Gamma_c(\delta, x_s)$ and the nonergodicity parameters are calculated with MCT.

In figure 5.1 Hajnal’s result for the glass transition surface is given. An interpretation of the results is presented in [14]. The surface has a plateau above the one-component boundary value. Only for small δ , Γ_c increases greatly towards the smurfy edge (the region with small δ and large x_s), similar to the system of hard disks. The boundary value of Γ_c is constant, so the value has to drop again for $x_s \rightarrow 1$. Nevertheless, because of crystallizing effects it was not possible to do simulations close enough to $x_s = 1$ to see the drop. For small δ , Γ_c seems to be linear over a long range of x_s . For the dipolar system the glass is stabilized by mixing for all configurations.

The structure data can be seen in fig. 5.2. The correlation is always stronger for the majority particle sort. The peaks in S shift to smaller k if x_s is increased.

F/S on the left hand side of the figure shows basically the same behavior as for hard disks.

A plot of the particle coordinates (see fig.5.3) shows that for intermediate x_s the system has a liquid-like configuration. For large δ there is some small-scale crystallizing visible. Here we can see an effect found by Hoffmann et al. [15]: The small particles form a sponge-like topology, whereas the larger ones form [crystallizing] clusters.

For small δ and large x_s – the smurfy edge – however, the big particles are evenly distributed, almost as one would expect in a gas (if the wave-like phenomenon is ignored that probably is produced by the periodic boundary condition).

5.2. Shear modulus

The shear modulus $G_\infty/(nk_B T)$ is calculated on the critical surface $\Gamma_c(x_s, \delta)$ with $x_s \in [0.1, 0.9]$ and $\delta \in [0.1, 0.6]$ As input it uses the structure data calculated by David Hajnal [14] for about 250 values of k .

For graphs of the results see 5.4. The limits for $x_s \rightarrow 1$ or $x_s \rightarrow 0$ or $\delta \rightarrow 1$ are the same (see 3.3). With the figures it can be estimated as 25, assuming the shear modulus grows monotonically toward the boundary like the shear modulus of the hard spheres instead of dropping down like Γ_c .

Mixing decreases the shear modulus in the whole regime of δ . For small δ the curve has a similar behavior but the minimum is lower and shifts to higher x_s . Unlike the other curves (the critical surfaces and the shear modulus of hard spheres), there is no different behavior in the smurfy region. It is not clear whether the shear modulus increases beyond the boundary value before reaching the boundary as in the hard sphere system, since simulation could only be done up to $x_s = 0.9$.

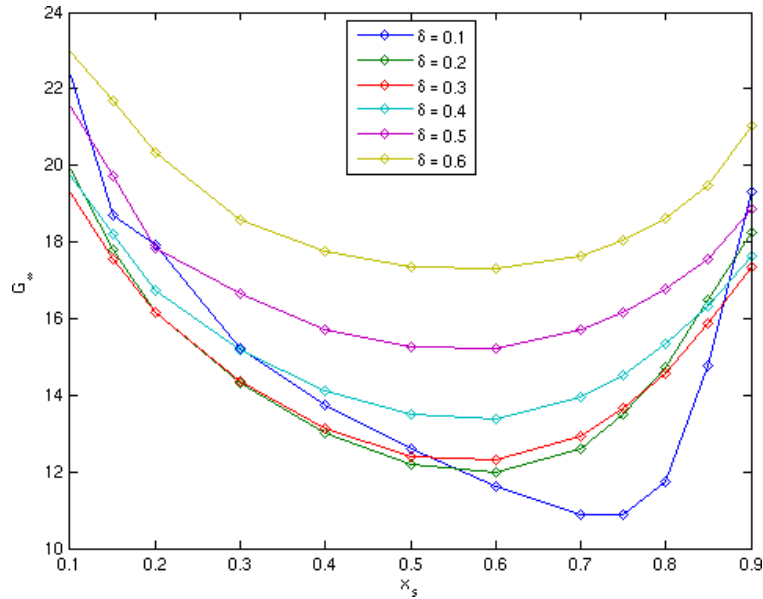


Figure 5.4.: Plateau shear modulus $G_{\infty}(x_s)$ for the dipolar system. Mixing plasticizes the system.

5.3. Comparison with experiment

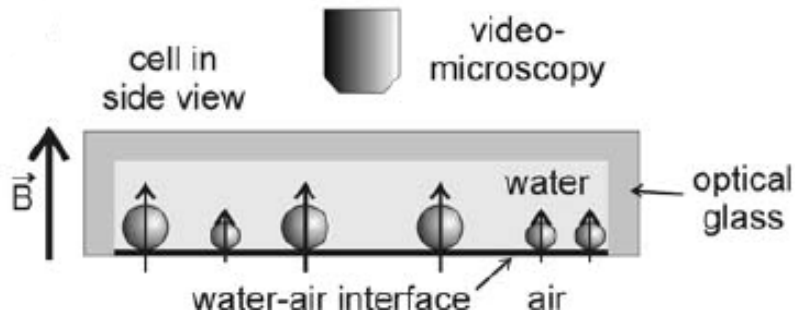


Figure 5.5.: Setup of the experiment [8]

Recently there have been measurements with the experimental system [8] to determine the glass transition by looking at the change in the plateau shear modulus when Γ is increased. According to MCT, this should jump from 0 to $G_{\infty} \neq 0$ at the glass transition.

From the experimental values [16] in fig. 5.6 with $\delta = 0.1$ and $x_s = 0.45$, the critical parameter Γ_c can be estimated as 220 or 330, depending on the interpretation which of two steps in the shear modulus is the glass transition. The experimental data is not directly measured but calculated using the equipartition theorem. The resulting formula for the plateau shear modulus is

$$\frac{G_{\infty}}{k_B T} = \lim_{\vec{q} \rightarrow 0} [q^2 \langle |u_{\perp}(\vec{q})|^2 \rangle]^{-1}$$

It is $G_{\infty}(\Gamma = 220)/(nk_B T) \approx 5$ and $G_{\infty}(\Gamma = 330)/(nk_B T) \approx 13$.

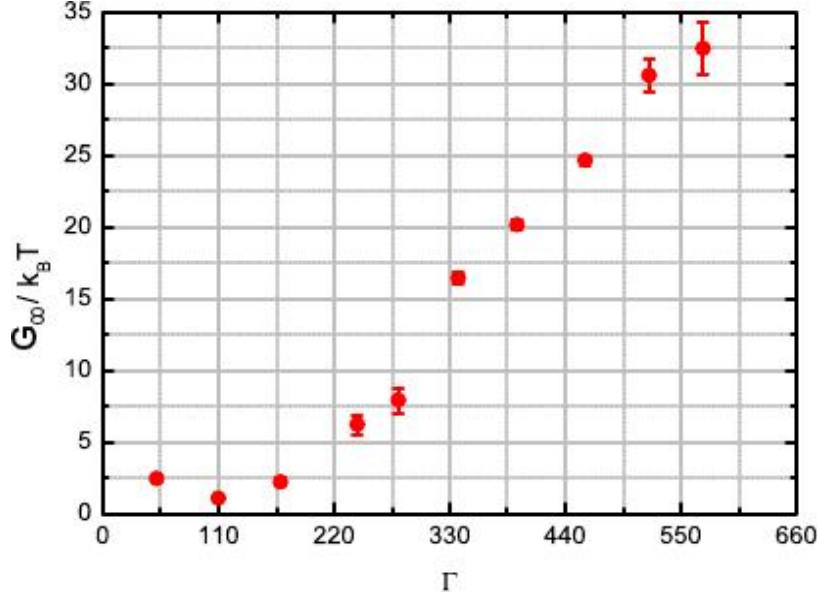


Figure 5.6.: Preliminary experimental values of $G_\infty = \mu(\Gamma)$ for $x_s = 0.45$, $\delta = 0.1$.

The numerical values calculated by David Hajnal and me are $\Gamma_c \approx 110$ and $G_\infty / (nk_B T) \approx 13$ (see 5.1 and 5.4). While the shear modulus is almost the same, the critical parameter is only one half of the experimental value. But differences in the critical parameter of about a half of its value are known for MCT for other systems [2].

This can be seen as evidence for a qualitative agreement between experiment and MCT.

5.4. Summary

The binary mixture of dipolar particles shows a stabilizing of the liquid through mixing, while the plateau shear modulus at the glass transition is lowered. Both are plasticizing effects that we have found for the three- and the two-dimensional system of hard spheres as well.

The comparison to the experimental system yields a qualitative agreement if the known MCT error of the glass transition parameter Γ is ignored. But since there are experimental values only for one configuration of the system, this is rather inconclusive.

6. Interpretation of the results

The main effects found for G_∞ are the same for hard spheres as well as for dipolar particles. Both systems show plasticizing for the mixture relative to the monodisperse system.

At first sight, there is a difference in the smurfy region – with small δ and large x_s – because the hard sphere system shows an increase in G_∞ , while for the dipolar system the region behaves similarly to the rest.

We will look at the plasticizing effect first, then at the smurfy region.

6.1. Perturbation of a mono-disperse system

We will try to explain the plasticizing effect as a perturbation of a mono-disperse system by the other sort of particles. Therefore, we calculate the shear modulus with the one-component formula but take one of the diagonal entries of structure data of the binary system, cf. 3.6 eq. (3.2). This should be the same as accounting for the other particles as an interaction term. We will add up both perturbation terms of the two sorts of particles, so that we can compare our perturbation results with the values calculated with the two-component equation (3.1). The resulting perturbation curve (see fig. 6.1) shows plasticizing as well. It also qualitatively reproduces the anomalous results for the smurfy edge, though overestimating them.

The limits at the boundaries seems to be roughly the same for perturbation and two-component calculation. They can be estimated as $G_\infty/(nk_B T) = 25$ for the dipolar system and 18 for the hard sphere system.

For $x_s \approx 0.5$ the values of perturbation and two-component calculation are surprisingly still similar. This gives the impression that the perturbation theory describes the system well. This might mean that the components act relatively independent and that each component only gives an interaction term to the other component.

The line of the hard sphere perturbation for $\delta = 0.9$, where G_∞ is increased through mixing, can be ignored. Here the particles are almost the same and so the small particles cannot be seen as a small perturbation.

However, at the boundaries where the perturbation method should produce the best results, we see some curvature that is not visible for the other calculation.

This leads to the question whether the MCT-formula is valid in these regions. A look at figure 5.3 (plots of the particle coordinates for the dipolar system) shows small-scale crystallizing for the configurations close to the boundary. But MCT assumes a homogeneous isotropic system. However, the plasticizing effect is visible throughout the whole regime and so is not effected by possible errors near the boundaries.

An explanation outside of MCT, especially for the regions close to the boundaries, for the plasticizing in the plateau shear modulus might be, that the particle sorts are independent and small crystallites in the mixture increase the shear modulus, which becomes bigger the

6. Interpretation of the results

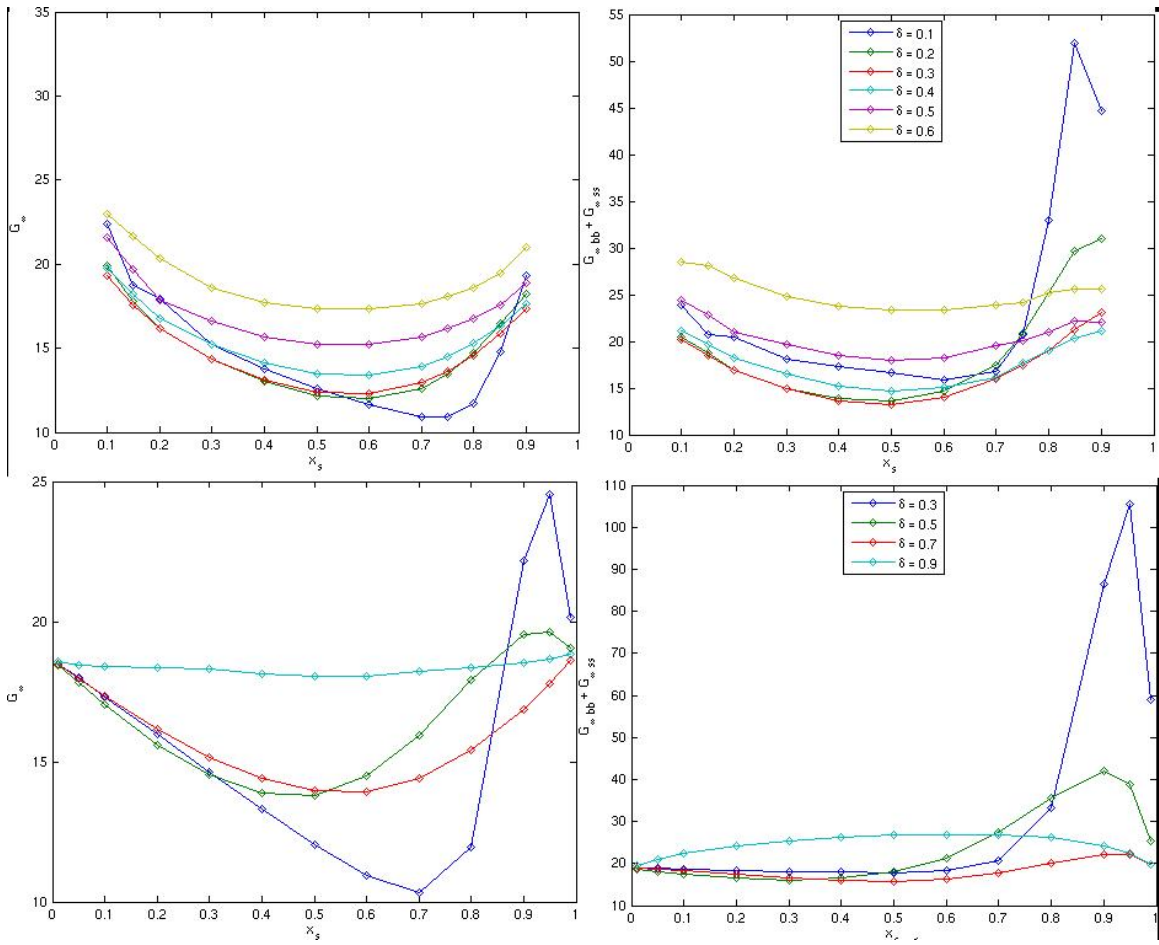


Figure 6.1.: G_∞ (left) and $G_\infty^{bb} + G_\infty^{ss}$ (right) for dipolar particles (top) and hard spheres (bottom).

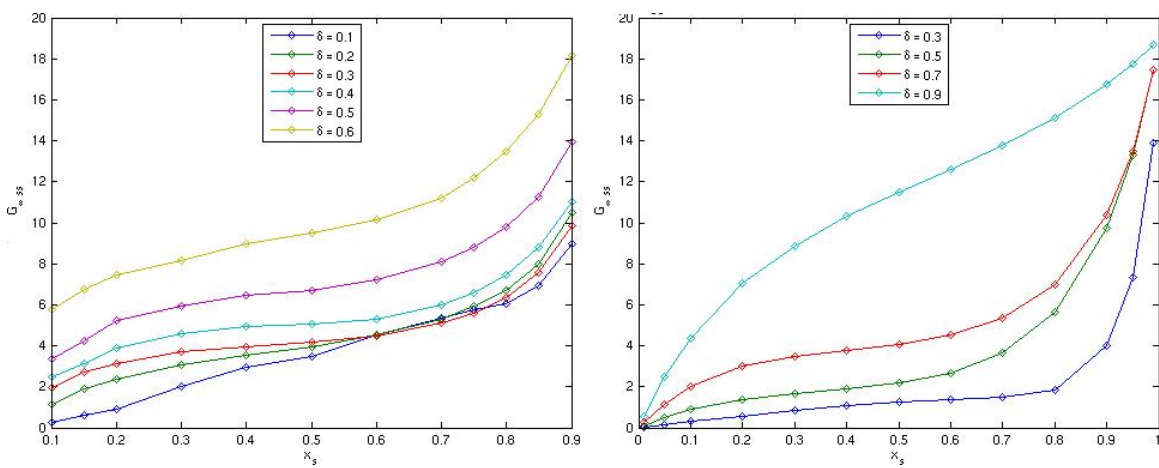


Figure 6.2.: G_∞^{ss} for dipolar particles (left) and hard spheres (right).

more and bigger crystallites exist. This would be sensible, since crystals are elastic, and so the shear modulus does not decrease a lot in time, so that the plateau shear modulus, which we calculate here, is quite big. By this theory, the main shear-decreasing factor would be the boundary-lines between different sorts of particles. Since the number of boundary lines increases for mixing, this is in accordance to the plasticizing effect.

6.2. Smurfy region

Especially the region with many very small particles deserves some thought. An increase of the shear modulus for $\delta \rightarrow 0$, $x_s \rightarrow 1$ can be seen for the hard sphere system before it drops again to the boundary value. It is not visible for the dipolar system, but the shear modulus rises steeper than elsewhere, and the region where the shear hardening is observed for hard spheres is not accessible for the Monte-Carlo simulation of dipolar particles because of crystallizing.

A plot of the particle coordinates for the dipolar system (fig.5.3) shows a differing configuration of the smurfy region from other compositions: The big particles are equidistantly spaced, but not – different from other configurations – without other particles in between. Instead, all the big particles are surrounded by small ones. So the smurfy region of the dipolar particles differs from the other regions as well, although this is not clearly visible for G_∞ .

Also both critical surfaces Φ_c and Γ_c have maxima in the smurfy region.

This raises the question, whether the maximum in the glass transition lines that is in the smurfy region for the hard sphere system in two and three dimensions, as well as for the dipolar system, can really be caused by an attraction-depletion force, as has been suggested for hard spheres [17].¹ But the dipolar particles have a repellent force and are point particles. So they should not show depletion effects, which is verified by the particle configuration in the bottom left panel in fig. 5.3.

The perturbation method gives a peak in the shear modulus for both systems. This is produced purely by the big spheres, as the small spheres show a monotonous increase from 0 at $x_s = 0$ towards the boundary value for $x_s = 1$ in figure 6.2. So we still get hints of a perturbative force of the small particles on the big ones, but this does not seem to be a depletion force.

¹The idea is that the small particles cannot be between close big particles, because there is not enough space and they are pressed out. Because of this, the density of small particles around the big ones is higher than between them and this creates an attractive force between the big particles.

7. Conclusion

In this thesis we have formulated an MCT equation to calculate the shear modulus for multi-component mixtures in two-dimensional systems.

With this equation and with structure data calculated with MC and MCT by Hajnal [7], we have calculated the plateau shear modulus for a binary mixture of hard spheres and for a binary mixture of dipolar particles in two dimensions at the glass transition. We have discussed the results, as well as the structure factors and the transition surface of the system's parameters. We could compare the results for the shear modulus with results of a perturbation calculation and with a three-dimensional system of hard spheres by Götze and Voigtmann [6]. For the dipolar system we also had experimental values for comparison by Klix [16] for the system developed by König et al. [8].

In the following we will summarize the effects seen for the two- and three-dimensional system of hard spheres and for the dipolar system.

We have found that in the region of small δ and large x_s that is here called the “smurfy region”, all systems have maxima in the critical surface (ϕ_c and Γ_c) as well as in G_∞ . (For G_∞ in the dipolar system this is not quite clear, but can nevertheless be assumed because of the perturbation calculation.) As a reason depletion attraction has been proposed [6] but this does not seem to fit here. A figure of the coordinates of the dipolar particles suggests rather the contrary. With the perturbation method it has been shown that the maxima in the plateau shear modulus are produced by the big particles and the force of the small ones on them.

With exception of the smurfy region, all systems show plasticizing (a lowering of G_∞ through mixing) through the whole mixing-regime. The plateau shear modulus $\frac{G_\infty}{nk_B T}$ has about the same size of 20 and variation of ± 10 for all systems.

The glass transition surface shows that for all systems the liquid is stabilized, but for the hard sphere systems there exists a threshold for δ above which the glass is stabilized. This threshold is lower for the two-dimensional system than for the three-dimensional one ($\delta < 0.5$ instead of $\delta < 0.8$).

A comparison with an experimental setup of the dipolar system shows a good agreement of the plateau shear modulus. The transition parameter Γ_c is overestimated by MCT by a factor of two or three, as has been found for other systems.

A perturbational method, where the shear moduli of the particles are calculated separately as would be done for a monodisperse system and then added up, shows good qualitative and mostly even quantitative agreements with the two-component calculation, although the maximum in the smurfy region is overestimated.

Overall MCT seems to yield good results for the systems studied here. Only close to the boundaries some small-scale crystallizing is visible in the particle plots of the dipolar system. In this region, the perturbation method and the two-component method give slightly differing results.

The effect of a decrease of the elastic moduli through mixing has also been found for

7. Conclusion

other systems. A polymer becomes softer when small particles are mixed into it. This is why we chose the name plasticizing to describe the phenomenon. A comparison can also be made to glass forming binary metal alloys, which can be described as hard spheres. There plasticizing has been observed as well.

This work shows that plasticizing – softening of the elastic moduli through mixture – is not only a polymer and hard sphere effect, but can be found for dipolar particles as well. It also shows that shear softening is not limited to three-dimensional systems but can also be found in two-dimensional systems.

Doubtlessly it can be interesting to compare the systems further so that one can see what other differences arise through the spatial dimension of the system. Especially the smurfy region might deserve some effort, to see if additional evidence for or against the depletion attraction can be found, as this thesis questions this theory.

An experiment with different x_s would be worth while, so that the MCT prognosis for the shear modulus could be tested more thoroughly. Another future project could be using the structure data of the experimental system to calculate the shear modulus with the MCT-formula.

A. Additional Figures in 3D rendering

Hard Spheres

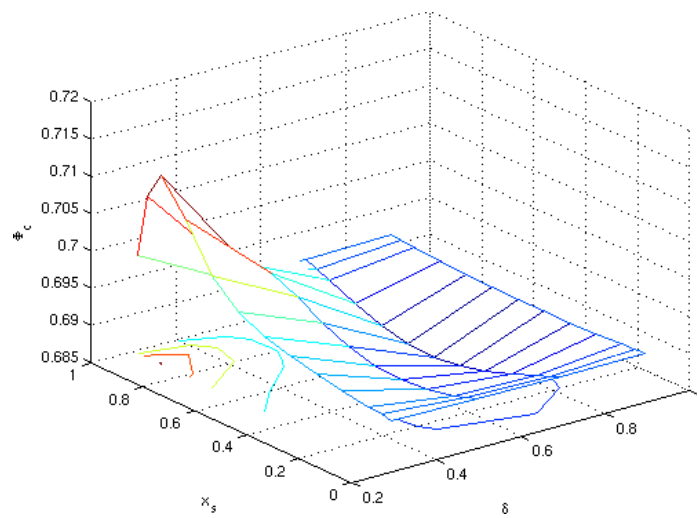


Figure A.1.: Hard disks: $\Phi_c(x_s, \delta)$. For the smurfy region (many small particles) the liquid is stabilized by mixing, everywhere else the glass.

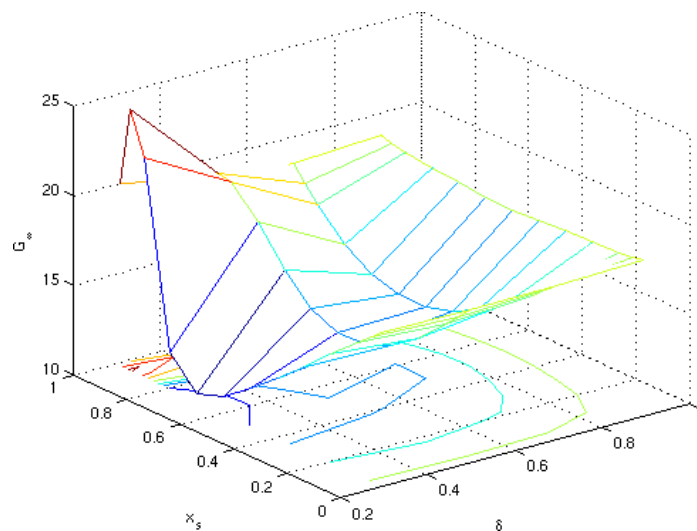


Figure A.2.: Hard disks: $G_\infty(x_s, \delta)$. Shear softening is observed except in the smurfy region.

Dipolar Particles

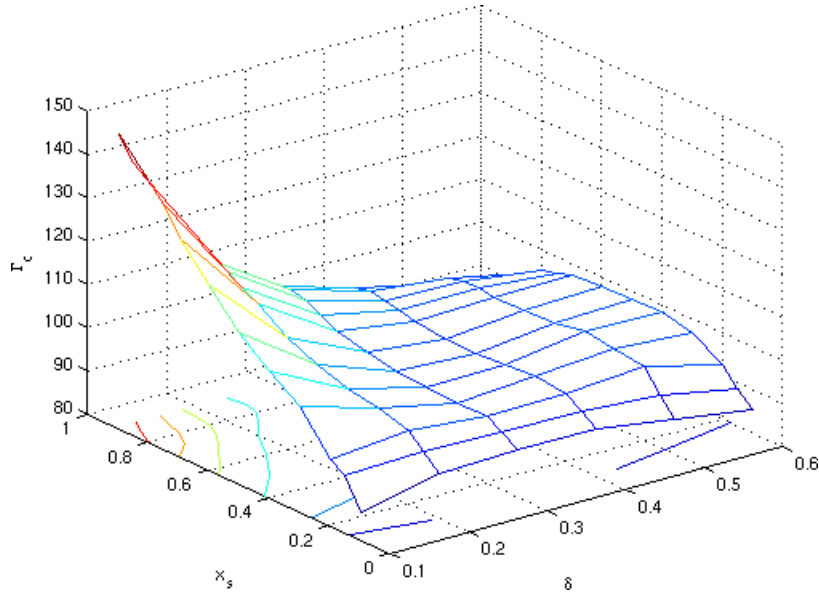


Figure A.3.: Dipolar particles: $\Gamma_c(x_s, \delta)$. The glass is stabilized by mixing.

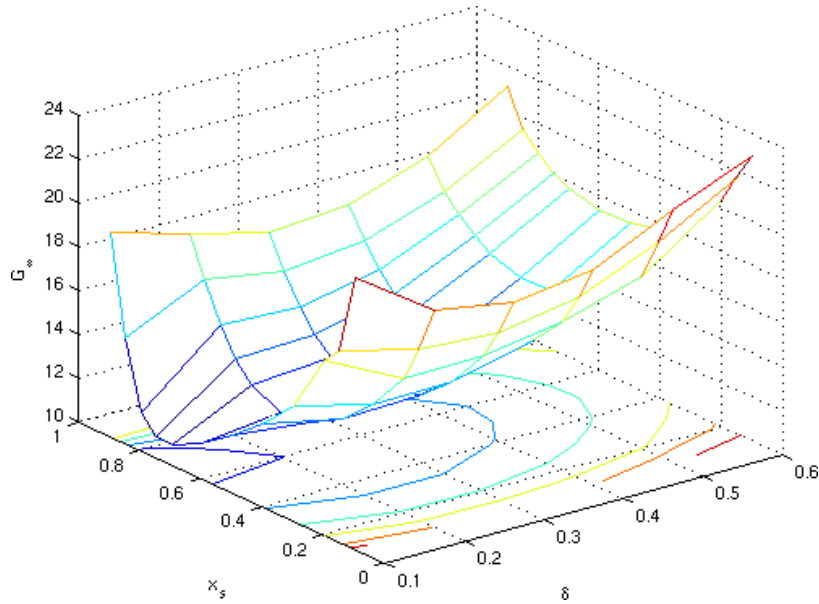


Figure A.4.: Dipolar particles: $G_\infty(x_s, \delta)$. Mixing shear softens the system.

Perturbation

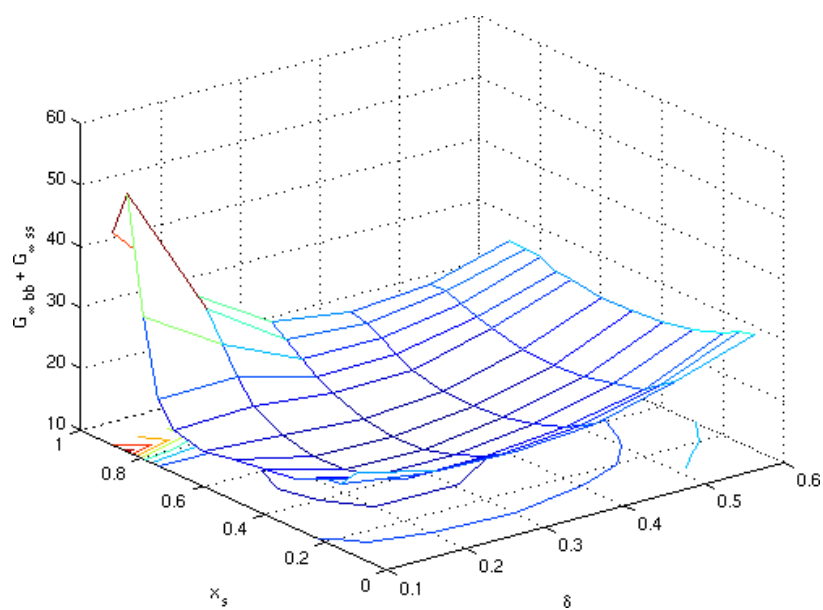


Figure A.5.: $G_{\infty}(x_s, \delta)$ for dipolar particles as sum of the perturbations of one sort of particles for dipolar particles.

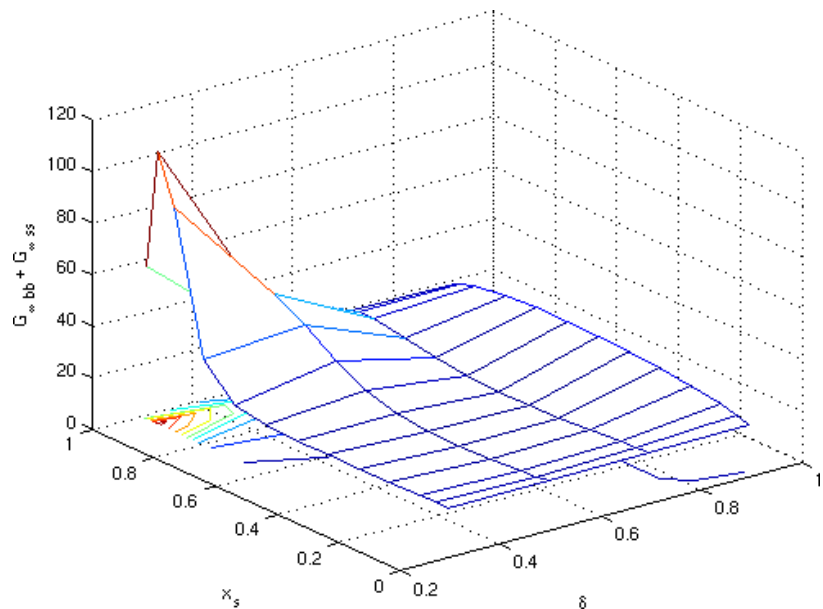


Figure A.6.: $G_{\infty}(x_s, \delta)$ for hard spheres as sum of the perturbations of one sort of particles for hard spheres.

Bibliography

- [1] U. Bengtzelius, W. Götze, and A. Sjölander. Dynamics of supercooled liquids and the glass transition. *Journal of Physics C: Solid State Physics*, 17(33):5915, 1984.
- [2] W. Götze. *Complex Dynamics of Glass-Forming Liquids, A Mode-Coupling Theory*. Oxford University Press, 2009.
- [3] T. Franosch, M. Fuchs, W. Götze, M. R. Mayr, and A. P. Singh. Asymptotic laws and preasymptotic correction formulas for the relaxation near glass-transition singularities. *Phys. Rev. E*, 55(6):7153–7176, Jun 1997.
- [4] B. Schmid and R. Schilling. Glass transition of hard spheres in high dimensions. *Phys. Rev. E*, 81(4):041502, Apr 2010.
- [5] M. Bayer, J. M. Brader, F. Ebert, M. Fuchs, E. Lange, G. Maret, R. Schilling, M. Sperl, and J. P. Wittmer. Dynamic glass transition in two dimensions. *Phys. Rev. E*, 76(1):011508, Jul 2007.
- [6] W. Götze and Th. Voigtmann. Effect of composition changes on the structural relaxation of a binary mixture. *Phys. Rev. E*, 67(2):021502, Feb 2003.
- [7] D. Hajnal. *Effect of Mixing, Particle Interaction, and Spatial Dimension on the Glass transition*. PhD thesis, Johannes Gutenberg-Universität Mainz, 2010.
- [8] H. König, R. Hund, K. Zahn, and G. Maret. Experimental realization of a model glass former in 2d. *The European Physical Journal E: Soft Matter and Biological Physics*, 18:287–293, 2005. 10.1140/epje/e2005-00034-9.
- [9] G. Nägele and J. Bergenholtz. Linear viscoelasticity of colloidal mixtures. *The Journal of Chemical Physics*, 108(23):9893–9904, 1998.
- [10] M. Fuchs. Notes on structure and correlation functions, density functional and mode coupling theory, and rheology, 2011.
- [11] M. Fuchs. Nonlinear rheological properties of dense colloidal dispersions close to a glass transition under steady shear. *Adv Polym Sci*, 236:55–115, 2009.
- [12] A. Wineman. Nonlinear viscoelastic solids—a review. *Mathematics and Mechanics of Solids*, 14(3):300–366, 2009.
- [13] F. Weysser and D. Hajnal. Tests of mode-coupling theory in two dimensions. *Phys. Rev. E*, 83(4):041503, Apr 2011.
- [14] D. Hajnal, M. Oettel, and R. Schilling. Glass transition of binary mixtures of dipolar particles in two dimensions. *Journal of Non-Crystalline Solids*, 357:302–310, 2011.

- [15] N. Hoffmann, F. Ebert, C. N. Likos, H. Löwen, and G. Maret. Partial clustering in binary two-dimensional colloidal suspensions. *Phys. Rev. Lett.*, 97(7):078301, Aug 2006.
- [16] C. Klix, F. Ebert, G. Maret, and P. Keim. Elastic properties of glasses.
- [17] S. Asakura and F. Oosawa. *J. Polym. Sci.*, 33(183), 1958.